Study on the Temperature Distribution in the First-Stage Turbine Blades of the TB3-117 Engine

Le Thanh Nguyen[#1], Duc Dung Nguyen[#2], The Son Nguyen[#3]
[#] Faculty of Aircraft - Engines, Air Force Officer's College, Khanh Hoa, Viet Nam
[1]thanhmbdc @gmail.com

Abstract:

In helicopter turboshaft engines, turbine blades operate under severe thermal and mechanical conditions. As engine power increases, the gas temperature downstream of the combustion chamber can reach approximately 1300 K, while high rotational speeds generate significant centrifugal forces. In addition, blades are exposed to non-uniform thermal and aerodynamic loads from hot gas flow, which strongly affect material properties. This study presents a numerical investigation of the temperature distribution in first-stage turbine rotor blades without internal cooling channels. The results identify regions of maximum temperature and assess blade durability. Comparison between numerical and theoretical results shows small temperature deviations: about 30°C at the tip, 8°C at mid-span, and 15°C at the root.

***Keywords*— Axial turbine, turbine blade, TB3-117 engine, temperature.**

I. INTRODUCTION

Helicopters equipped with turboshaft engines are capable of vertical takeoff and landing, hovering, and backward flight. Turboshaft engines have had a significant impact on the aviation industry by providing the required power output with minimal weight. The turbine is a critical component of the turboshaft engine. It can rotate at speeds of up to 20,000 rpm (reaching 19,540 rpm during takeoff [1]), thereby being subjected to substantial centrifugal forces. In addition, the turbine is exposed to extremely high gas temperatures downstream of the combustion chamber, which can reach up to 1300 K [6].

Turbine blades frequently experience various types of damage during engine operation, such as thermomechanical fatigue leading to cracking (Fig. 1), localized burning, corrosion damage (Fig. 2), and burn-through regions (Fig. 3). Figure 1 [7] illustrates a crack at the tip of a high-pressure turbine blade in an area without cooling holes. These cracks are caused by excessively high gas temperatures acting on the blade tip downstream of the combustion chamber, resulting in localized high temperatures at these locations. Ultimately, this leads to degradation of the microstructure of the material used in the first-stage high-pressure guide vane.

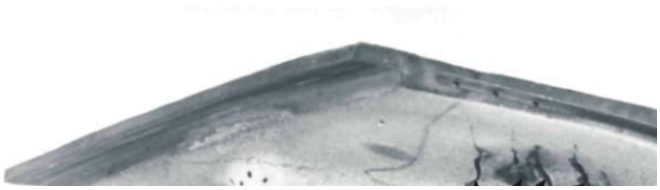

Fig. 1. Cracked regions on the turbine nozzle blade [6]

The combined effects of temperature, stress, and an oxidizing environment lead to diffusion processes in the surface layers of the blade, thereby limiting their durability [8]. When the fuel–air mixture combusts, it generates a gas flow characterized by high pressure, high temperature, and high velocity. In addition, turbine blades are subjected to significant stresses from centrifugal and aerodynamic forces, as well as exposure to the harsh environment of combustion products and atmospheric air. Protective properties may be reduced due to corrosion caused by high-temperature gases during operation.

Shown in Fig. 2 [9] is erosion–corrosion damage at the blade leading edge, resulting from repeated impacts of solid particles, which lead to mechanical degradation of the protective coating. A high carbon content in the fuel increases the corrosive effects of the gas flow, accelerating coking processes on components and sulfide corrosion, thereby amplifying the overall destructive impact.

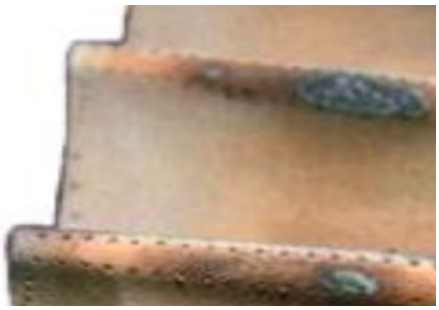

Fig. 2. Erosion–corrosion damage at the leading edge of the high-pressure turbine blade [9]

Unfortunately, our country currently lacks the capability to manufacture gas turbine engines or their replacement components, particularly turbine parts. Therefore, when a turbine blade is damaged, the entire turbine assembly may need to be replaced, resulting in significant costs [1]. The calculation of blade temperature distribution serves as a fundamental basis for determining turbine blade durability and improving the blade thermal field.

During engine operation, the continuous combustion of fuel generates high-temperature and high-pressure flows that

 ISSN: 3107-6513

directly impact the turbine blades. As a result, the blades are subjected to mechanical stresses due to aerodynamic and centrifugal forces and are degraded by chemical corrosion. In addition, to identify the causes of blade damage, it is necessary to determine the thermal state, particularly in the case of blades lacking internal cooling channels. Accurate calculation of temperature distribution is therefore essential for assessing the degradation of blade material properties.

II. NUMERICAL MODEL

There are various software packages available for calculating fluid dynamics and blade temperature distribution, including ANSYS CFX, STAR-CCM+, NUMECA, and Fluent. However, for this work, the ANSYS CFX module [13] was selected due to its advanced algorithms, which provide reliable, fast, and accurate solutions [12]. This software is well parallelized and offers a wide range of physical models capable of describing nearly all phenomena related to fluid flow. In this study, the ANSYS CFX module (ANSYS 2023 R1) was used to simulate the fluid dynamics in the flow path of the first-stage turbine rotor of the TB3-117 turboshaft engine.

The computational procedure employed in this study is illustrated in Fig. 3.

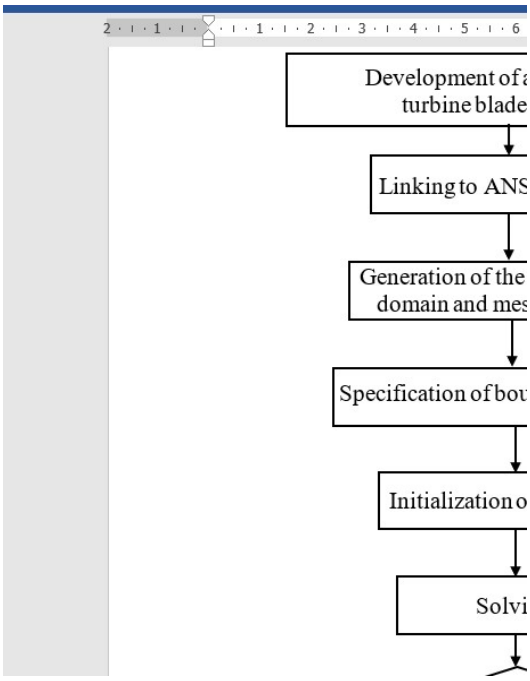

Fig. 3. Computational algorithm flowchart for the simulation problem

It is important to note that these blades are not internally cooled; therefore, the gas temperature has a significant influence on their operating conditions. Subsequently, the temperature distribution is calculated and used as input conditions to determine the stress field using the steady-state thermal analysis module. The one-way Fluid–Structure Interaction (FSI) approach (Fig. 4) enables a comprehensive analysis of the thermal and mechanical responses of the turbine blades (Fig. 5).

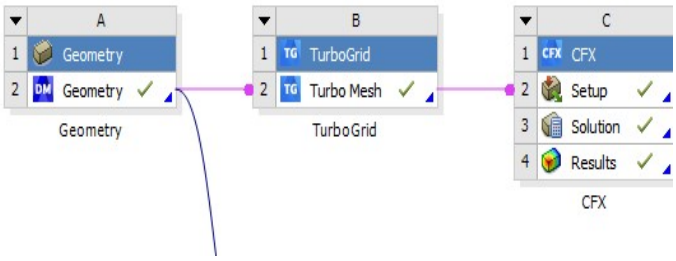

Fig 4. Computational model for turbine blade temperature distribution.

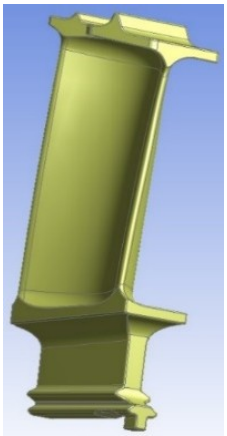

Fig 5. Turbine blade of the TB3-117 turboshaft engine.

When performing CFD calculations for the turbine gas path, hexahedral elements are recommended. In this study, the computational mesh was generated using the TurboGrid module. However, to accurately capture the detailed physical phenomena near the boundary layers between the turbine blades and the gas flow, a mesh refinement process was applied (Fig. 6).

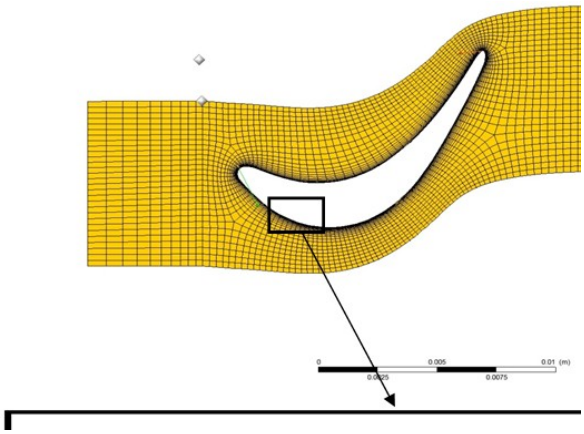

Fig 6. Blade cross-section mesh generated using the TurboGrid module.

The boundary conditions were set according to the takeoff operating parameters, as shown in Fig. 7, which represent the most critical operating regime of the engine, based on technical documentation . The following boundary conditions were applied: the inlet total pressure was 887,120 Pa, the inlet total temperature was 1,188 K, the turbine rotational speed was 19,540 rpm, and the outlet static pressure was 591,413 Pa [5]. The working fluid was assumed to be an ideal gas, and the simulation was performed under energy-conserving flow conditions with an appropriate turbulence model. The convergence criterion was set to 1×10^{-4}, or a

 ISSN: 3107-6513

minimum root mean square (RMS) residual of 1%, with the maximum number of iterations limited to 500 [7].

It can be observed that when the number of mesh nodes increases from approximately 105,000 to nearly 235,000, the total pressure downstream of the turbine blade changes only slightly. For computational efficiency, the authors selected a mesh consisting of 174,086 nodes and 159,720 elements for the simulations. This mesh resolution is considered acceptable and suitable for subsequent analyses.

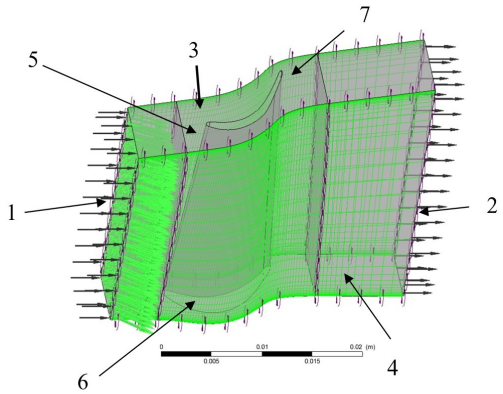

Fig. 6. Boundary conditions at:
1. Inlet; 2. Outlet; 3. Shroud; 4. Hub; 5. Blade profile; 6,7. Periodic surfaces

To analyze the steady-state thermal conditions and use the obtained results for calculating the temperature distribution of the turbine blade in the Steady-State Thermal Analysis module, a thermal analysis was conducted. This analysis evaluates the thermal equilibrium state of the system, in which the temperature remains constant over time. In other words, it assesses the equilibrium condition of a system subjected to constant thermal loads and environmental conditions [14]. In this module, the mesh was generated with 149,532 nodes and 85,081 elements, as shown in Fig 8. From the CFX simulation results, the convective heat transfer coefficient was extracted and applied as a boundary condition for the Steady-State Thermal Analysis, as illustrated in Fig 9.

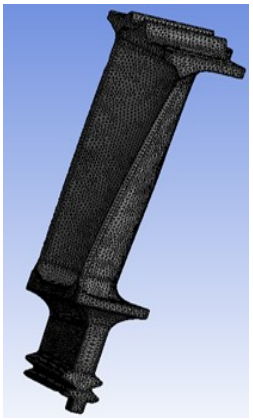

Fig. 8. Mesh model of the turbine blade.

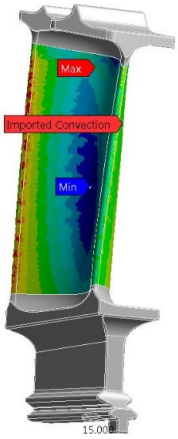

Fig. 9. Boundary conditions in the Steady-State Thermal Analysis module, represented by the applied convective heat transfer coefficient.

The alloy used for the turbine blades of the TB3-117 turboshaft engine is a heat-resistant and corrosion-resistant material, with properties equivalent to XH77TIOP steel (NiCr20TiAl). The chemical composition of the material was defined and imported into the Engineering Data module for the steady-state thermal analysis.

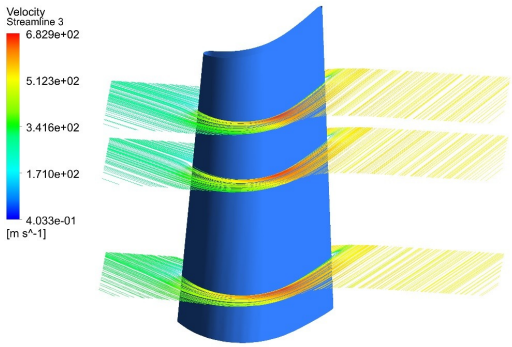

Fig 10. Distribution of low flow velocity along the blade span

The flow velocity gradually increases from the turbine inlet to the outlet, as illustrated in Fig 10. This behavior is attributed to the conversion of a portion of the internal energy, particularly enthalpy, into kinetic energy as the working gas expands through the turbine passage. The observed increase in flow velocity is therefore a direct consequence of this energy transformation process. The obtained velocity distribution is in good agreement with the fundamental theory of gas turbine engines [14], confirming the validity of the numerical results and their suitability for subsequent thermal and structural analyses.

The gas temperature acting on the turbine blade varies along the blade surface, as shown in Fig 11. The high-temperature region on the blade cross-section gradually decreases from the leading edge toward the trailing edge. The maximum temperature is observed at the leading edge and the blade shroud region, while lower temperatures are recorded toward the trailing edge. This temperature distribution reflects the direct exposure of the leading edge to the high-temperature combustion gases and the progressive heat transfer along the blade surface.

 ISSN: 3107-6513

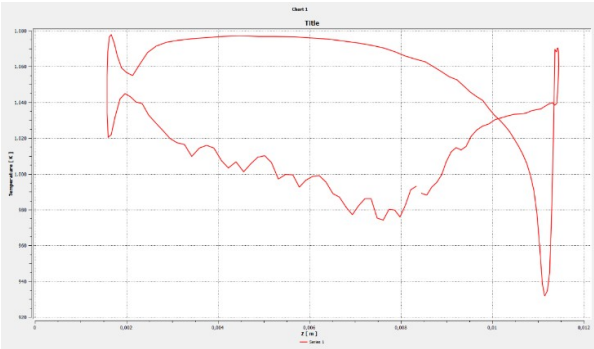

Fig 11. Temperature distribution on the mid-span cross-section of the turbine blade

Figures 12, 13, and 14 illustrate that the leading edge of the turbine blade is exposed to a significant amount of thermal load directly from the hot gas flow, reaching a maximum temperature of approximately 1077 K. Consequently, during engine operation, particular attention must be paid to the upstream gas temperature of the turbine in order to prevent blade overheating and potential thermal damage. These findings are consistent with the calculation results reported in previous studies , confirming the reliability of the numerical approach adopted in this work [15]. As shown in Fig. 15, the temperature distribution along the blade surface is highly non-uniform, with the highest temperature of 1048.5 K observed near the blade tip. In addition, the leading edge exhibits localized high-temperature regions, indicating critical thermal zones that are particularly susceptible to thermal fatigue and material degradation.

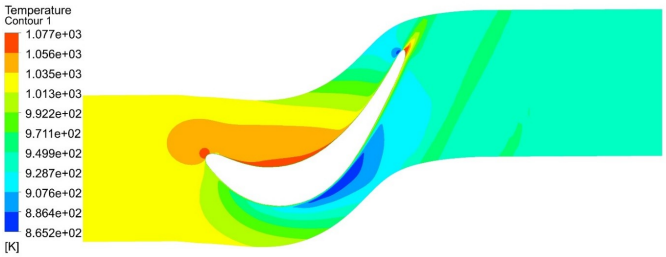

Fig 12. Temperature distribution on the mid-span cross-section of the turbine blade

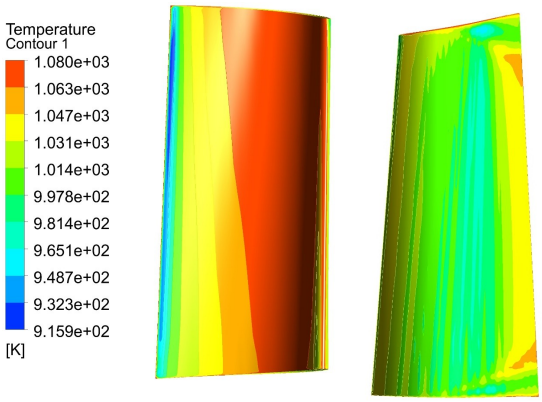

Fig 13. Temperature distribution curve along the turbine blade

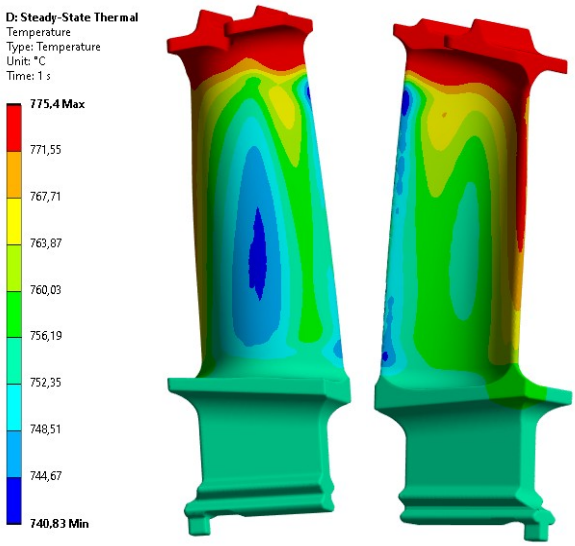

Fig 14. Temperature distribution over the turbine blade surface

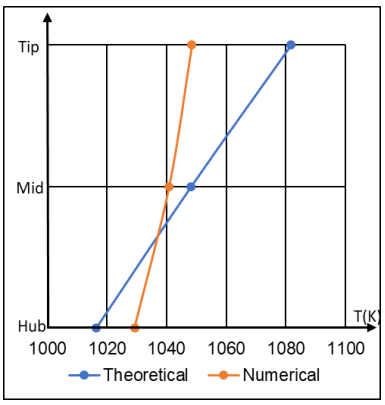

Fig 15. Comparison between theoretical results and numerical simulation results

Fig 15 presents a comparison between the numerical and theoretical results. According to the theoretical analysis, the temperature along the turbine blade increases steadily from the hub to the tip. However, the numerical results indicate a more gradual increase in blade temperature from the hub toward the tip. This behavior is attributed to the non-uniform temperature distribution of the gas flow. In particular, at the hub region, the numerical results predict a higher temperature compared to the theoretical values, whereas at the blade tip, the numerical temperature is lower than that obtained from theoretical calculations. Nevertheless, the discrepancies between the two approaches remain relatively small. For example, the temperature differences at the hub, mid-span, and tip are approximately 15,8 K, and 30 K, respectively. Such deviations are considered acceptable for subsequent calculations aimed at determining the stress field and structural strength of the turbine blade.

III. CONCLUSIONS

This study confirms that the upstream combustion gas has a significant impact on the first-stage turbine blades, particularly those without internal cooling channels.

The numerical results obtained using ANSYS software show good agreement with theoretical calculations and fall

within acceptable deviation limits. The analysis indicates that the leading edge of the blade experiences the highest temperature. Furthermore, due to the high rotational speed during engine operation, the turbine blades are subjected to considerable mechanical loads. Consequently, temperature plays a crucial role in determining the safe operating limits of the blades, which directly affects the overall technical condition of the engine.

Therefore, the selection of appropriate blade materials during the engine design phase is of critical importance to ensure stable operation and optimal performance, while minimizing the risk of catastrophic engine failure. This study provides a basis for evaluating the safety factor of turbine blades at different cross-sections and for investigating the temperature distribution along the blade. Based on these findings, design improvements can be implemented to enhance engine service life, thereby improving the overall durability and reliability of the engine.

REFERENCES

[1] Bogdanov, N.P., Kalinin, A.I., Krivo, A.I. (2000). *TB3-117 Turboshaft Engine*. Air Transport Publishing House, Russia. (in Russian)

[2] Catana, R.M., Dediu, G., Tarabic, C.M. (2022). Numerical and experimental investigation for evaluating the operating regime of the TV2-117A turboshaft engine. *Applied Sciences*, 12, 3703. https://doi.org/10.3390/app12073703

[3] Kurzke, J. (2005). How to build a performance model of a gas turbine from limited information. In *Proceedings of ASME Turbo Expo 2005: Power for Land, Sea and Air*, Reno, NV, USA, June 6–9, 2005. ASME GT2005-68537, pp. 145–153. https://doi.org/10.1115/GT2005-68536

[4] Chapman, J.W., Lavelle, T.M., Litt, J.S. (2016). *Practical techniques for modeling gas turbine engine performance*. NASA/TM-2016-219147, Glenn Research Center, Cleveland, OH, USA.

[5] Klimov Design Bureau (1986). *Technical Manual of the TB3-117 Aircraft Engine*. Klimov Institute, Russia. (in Russian)

[6] Inozemtsev, A.A., Sandratski, V.L. (2006). *Gas Turbine Engines*. UEC-Aviadvigatel, Russia. (in Russian)

[7] Petrova, M.A., Saadatibai, M., Tarasov, A.I. (2015). Analysis of operating conditions of surface layers in modern gas turbine engines. *Civil Aviation High Technologies*, pp. 124–127.

[8] Meher-Homji, B., Gabriles, G. (1995). Gas turbine blade failures—Causes, avoidance, and troubleshooting. In *Proceedings of the 27th Turbomachinery Symposium*, pp. 129–180.

[9] Luo, L., Yan, H., Du, W., Hou, L., Fu, Y., Wang, S. (2023). Numerical analysis of film cooling characteristics of trenched holes under rib-disturbed supply flow and curved surfaces. *Physics of Fluids*, 35(3), 036105. https://doi.org/10.1063/5.0142276

[10] Wu, C., Yang, X., Tang, X., Ding, J., Weng, P. (2023). Numerical investigation of flow mechanisms and heat transfer in wavy cooling channels of turbine blades. *Physics of Fluids*, 35(2), 026105. https://doi.org/10.1063/5.0137217

[11] Kumar, A., Pathak, M. (2023). Conjugate heat transfer analysis of internally cooled superalloy turbine blades with rib-roughened channels. *Physics of Fluids*, 35(9), 095112. https://doi.org/10.1063/5.0165561

[12] Phan, H.M., Duan, P.H., Dinh, C.T. (2020). Numerical aero-thermal investigation of high-pressure turbine nozzle guide vanes: Effects of inlet flow conditions. *Physics of Fluids*, 32(3), 034111. https://doi.org/10.1063/1.5144418

[13] ANSYS Inc. (2023). *ANSYS Mechanical User's Guide*. ANSYS Inc., USA.

[14] Walsh, P.P., Fletcher, P. (1998). *Gas Turbine Performance*. Blackwell Science, USA.

[15] Rogers, G.F.C., Saravanamuttoo, H.I.H., Mayhew, Y.R. (1996). *Gas Turbine Theory*, 4th ed., Longman Group Limited, London, UK.